Chapter 6

Numerical solution of Euler equations with gravity using HLLC method

6.1 Introduction

Conservation laws accompanied with gravitational source term can be seen in many PDE models such as shallow water equations and Euler equations with gravitation. Euler equations with gravity are very useful in the mathematical modeling of atmospheric flows and stellar structure simulations in astrophysical phenomena. In real life situations, the Euler equations with gravity include source term, that is, terms that are functions of the unknown vector. For the solution of this problem efforts have been made to develop the best method for the handling of source term. This resulted in the development of a wide range of well balanced and non-hydrostatic numerical schemes. The main theme of well balanced scheme is based on the preservation of the motionless steady state or the hydrostatic reconstruction of solutions.

Well balanced schemes for Euler equations with gravity were developed using the relaxation schemes of Berthon et. al. (2014, 2016), in which an approximation of the hydrostatic solution is incorporated in the approximate Riemann solver. Guillard et al. (1999) studied the properties of upwind schemes in low Mach number limits. Ismail et al. (2009) discussed the flux functions which are entropy consistent at the shock. Xing and Shu (2013) presented a well balanced finite volume weighted essentially non oscillatory (WENO) scheme for Euler equations with gravity. Kappeli and Mishra

(2014) presented a second order well-balanced scheme that uses hydrostatic reconstruction for an isentropic flow with general equation of state. It can be seen in Landau and Lipschitz (1987) that an isentropic hydrostatic atmosphere is only neutrally stable. Leveque (2011) used the path integral method to formulate a wave propagation algorithm that is well-balanced for isentropic solutions. Leveque and Bele (1999) extended the path integral to obtain well balanced solutions of isothermal equations. Fuchs et al. (2010) developed a well balanced numerical scheme for ideal, compressible, MHD equations with constant gravitational acceleration for non isothermal hydrostatic solutions. Luo et. al. (2011) derived a well-balanced gas-kinetic scheme for isothermal stationary solutions of flow under gravitational field. Using the source term formulation of Xing et. al. (2013), Touma et. al. (2016) developed a non staggered central scheme which is well balanced for isothermal stationary solutions of Euler equations with gravity. For shallow water equations with variable bottom geometry, different numerical solutions to the Riemann problem have been suggested in Alcrudo et. al. (2001), Chinnayya et. al. (2004), Lefloch et. al. (2007), Bernetti et. al. (2007), Rosatti et. al. (2010) and Lefloch et. al. (2011). All the numerical schemes discussed above were constructed to devise a good balance in case of steady state equilibrium retaining as valid approximate solutions obtained in the basic works of Roe (1981) and Harten et. al. (1983). The occurrence of source term affects the characteristics of the exact solution, see Shu et. al. (1988), Toro at. Al. (1994) and Gupta et. al. (2016). The existence of source term modifies the solution of the Riemann problem, and the characteristic constant defined for the case when source term is absent in Godunov (1959) and Roe (1981) is no longer valid. Thus, the presence of source term creates problem in the correct numerical simulation of the model under consideration.

Another approach is to use operator splitting procedure for the treatment of source term. It is shown in Chen et. al. (2004) that, the solution of shallow water equations with operator splitting converges to the exact solution. Here the one dimensional conservation equations with source term are broken into two parts. The first part consists of the conservation law problem and the second part consists of the transient problem. For the numerical solution of conservation laws, the paper of Godunov (1959) was the initial landmark for the construction of most widely used numerical schemes. The Godunov type method uses the solution of local Riemann problem at the cell interfaces. Following the Roe method (1981), The HLL method (1983) developed by Harten et. al. is the most disseminated approximate Riemann solver. In the HLL method the fluxes at cell interfaces are approximated under the assumption that the intermediate state is bounded by two waves. When the hyperbolic system has more than two equations, there are more waves in the solution, which has to be taken care of. For the resolution of this problem Toro et al. (2009) proposed the introduction of contact discontinuity that resulted in the HLLC method. The HLLC method has the ability to resolve contact discontinuities.

In the present work, the numerical solution of Euler equations with gravity is obtained using the HLLC scheme for the numerical calculation of fluxes. The source term has been treated using the operator splitting procedure. The discontinuity due to source term is assumed at the cell interfaces. The method is then applied on some test problems. The numerical results show a close agreement between our non-hydrostatic scheme and the earlier well balanced schemes.

6.2 Governing equations

The system of one dimensional Euler equations governing the conservation of mass, momentum and energy of an inviscid, non-heat conducting fluid with static gravitational potential are given by

$$\begin{aligned}
&\frac{\partial \rho}{\partial t}+\frac{\partial}{\partial x}(\rho u)=0,\\
&\frac{\partial(\rho u)}{\partial t}+\frac{\partial}{\partial x}(p+\rho u^2)=-\rho\frac{\partial \phi}{\partial x},\\
&\frac{\partial E}{\partial t}+\frac{\partial}{\partial x}(E+p)u=-\rho u\frac{\partial \phi}{\partial x}.
\end{aligned} \tag{6.1}$$

Here ρ denotes the fluid density, u the velocity, p the pressure, E the total energy per unit volume excluding the gravitational energy, and ϕ is the time independent gravitational potential. The pressure is given by

$$p=(\gamma-1)[E-\frac{1}{2}\rho u^2], \quad \gamma=\frac{c_p}{c_v}, \tag{6.2}$$

where γ is the ratio of the specific heats at constant pressure and volume, taken to be constant.

In compact notation the system of equations (6.1) can be written as

$$\frac{\partial U}{\partial t}+\frac{\partial F}{\partial x}=S(U), \tag{6.3}$$

with

$$U=\begin{pmatrix}\rho\\ \rho u\\ E\end{pmatrix},\ F=\begin{pmatrix}\rho u\\ p+\rho u^2\\ (E+p)u\end{pmatrix},S=\begin{pmatrix}0\\ -\rho\,\partial\phi/\partial x\\ -\rho u\,\partial\phi/\partial x\end{pmatrix}, \tag{6.4}$$

where U is the vector of conserved variables, F is the corresponding flux vector and S is the vector of source terms. The Jacobian matrix for the convective part is given as

$$A = \frac{dF}{dU} = \begin{bmatrix} 0 & 1 & 0 \\ \frac{1}{2}(\gamma-3)u^2 & (3-\gamma)u & \gamma-1 \\ \frac{1}{2}(\gamma-2)u^3 - \frac{\gamma pu}{\rho(\gamma-1)} & \frac{3-2\gamma}{2}u^2 + \frac{\gamma p}{\rho(\gamma-1)} & \gamma u \end{bmatrix}. \tag{6.5}$$

The convective part is strictly hyperbolic with eigenvalues $\lambda_1 = u-a, \lambda_2 = u, \lambda_3 = u+a$, where $a = \sqrt{\gamma p/\rho}$. The right eigenvectors corresponding to the eigenvalues are

$$e^1 = \begin{bmatrix} 1 \\ u-a \\ H-ua \end{bmatrix}, e^2 = \begin{bmatrix} 1 \\ u \\ u^2/2 \end{bmatrix}, e^3 = \begin{bmatrix} 1 \\ u+a \\ H+ua \end{bmatrix}, \tag{6.6}$$

where H is the enthalpy given as $H = (E+p)/\rho$.

6.3 One dimensional flow and Riemann problem

To obtain the numerical solution of the system, a computational domain [0, L] of length L is considered. The domain is divided into cells of constant length size Δx, the i^{th} cell is given by $[x_{i-1/2}, x_{i+1/2}]$ with $x_{i+1/2} = i\Delta x$ and the position of the center of the cell I is given by $(i-1/2)\Delta x$. Let Δt be the time step size and $t^n = n\Delta t$ a generic time; the cell-average value of the solution $U(x,t)$ for the ith cell at time t^n is indicated by U_i^n , i.e.,

$$U_i^n = \frac{1}{\Delta x}\int_{x_{i-1/2}}^{x_{i+1/2}} U(x,t^n)dx \ , \tag{6.7}$$

Thus, U_i^n is a piecewise constant approximation of the solution at time t^n .

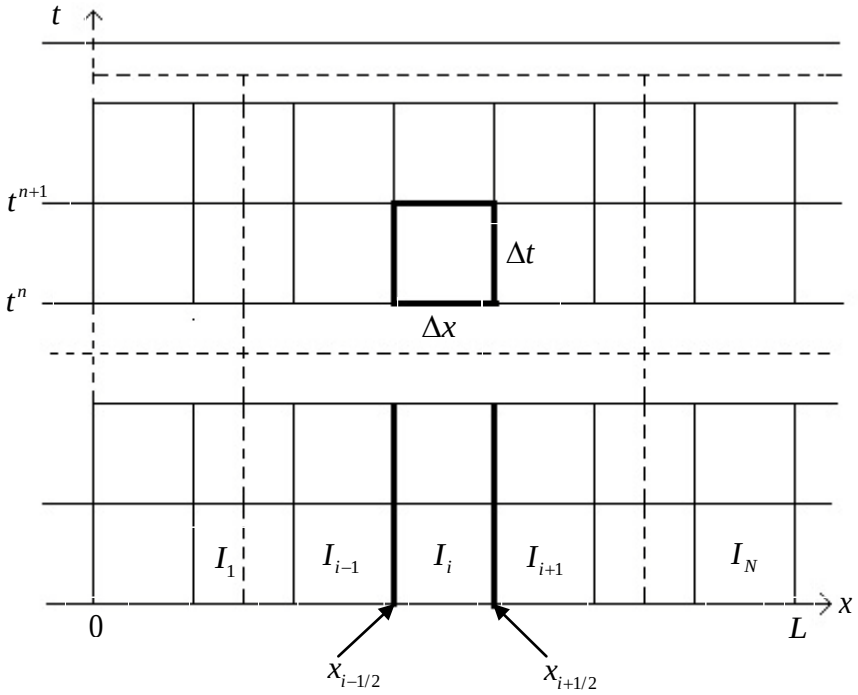

Figure 6.1 The grid discretization in the x-direction.

Consider the initial value problem for the system

$$\frac{\partial U}{\partial t}+\frac{\partial F}{\partial x}=S(U), \tag{6.8}$$

with the following initial conditions at each $i+1/2$ edge

$$U(x,0)=\begin{cases}U_i & \text{if } x<0,\\ U_{i+1} & \text{if } x>0.\end{cases} \tag{6.9}$$

The Riemann problem for Euler equations, abbreviated as *RP* is a problem involving two separate states say U_i^n and U_i^{n+1}. At the point $i+1/2$, the interface of the cells i and $i+1$, there is an initial discontinuity due to the fact that state variables on either side of this point are different. The solution to this $RP(U_i^n, U_i^{n+1})$ results in three waves emanating from the point $x_{i+1/2}$, corresponding to the eigenvalues of the Jacobian matrix given as $\lambda_1=u-a, \lambda_2=u, \lambda_3=u+a$, where $a=\sqrt{\gamma p/\rho}$. Out of these, the left and right waves can be shock or rarefaction indifferently whereas the middle one is always a

contact discontinuity. The figure 6.2 represents a typical Riemann problem with initial data states U_L and U_R. The region U_L lies to the left of the left wave, while U_R lies to the right of the right wave. The region in between the waves of speed S_L and that of speed S_R is depicted by the star region with U_L^* and U_R^*, the regions to the left and right of the contact discontinuity respectively. The solution to the given Riemann problem may lie in any of the four regions considered above based on the position of the point at which the solution is sought. This solution can be calculated using the exact mathematical method, which are time consuming or can be approximated by using approximate Riemann solvers, which are computationally efficient and gives better results with Godunov type methods. In the present case, the given Riemann problems, $RP\left(\mathrm{U}_i^n, \mathrm{U}_{i+1}^n\right)$, $RP\left(\mathrm{U}_{i-1}^n, \mathrm{U}_i^n\right)$ are solved using the HLLC approximate Riemann solver which takes into account the contact wave present in the solution.

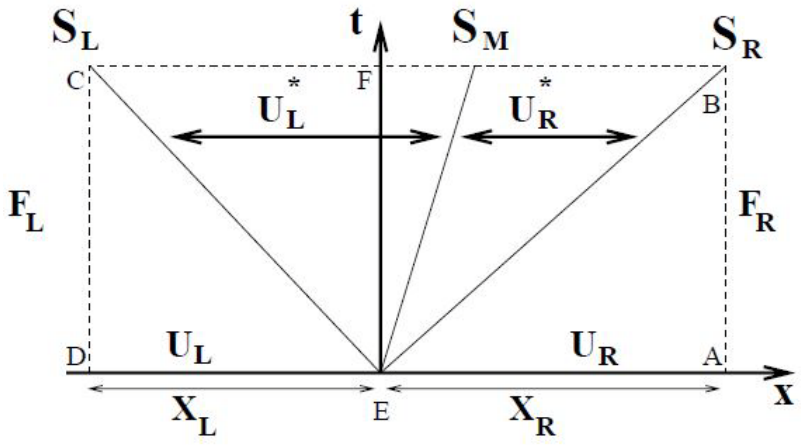

Figure 6.2 Wave structure in the solution of Riemann problem

However, the presence of source term in the problem modifies the solution of the Riemann problem. The solution may not preserve the wave structure of the Riemann problem obtained in the absence of source term.

6.4 Method of solution

The hyperbolic system of conservation law with source term

$$U_t + F(U)_x = S(U) \ , \tag{6.10}$$

can be simplified as the homogeneous problem by considering no source term

$$U_t + F(U)_x = 0 \ . \tag{6.11}$$

Another simplification results by considering that there are no spatial variations.

$$\frac{dU}{dt} = S(U) \ . \tag{6.12}$$

There are essentially two approaches to solve the inhomogeneous systems of the form (6.10), see Toro (2009). One approach is to preserve some coupling between the two processes in (6.10). These two processes might be represented by the systems (6.11) and (6.12). Another approach is to split (6.10) into homogeneous problem (6.11) and source problem (6.12). Here we follow the second approach.

The hyperbolic conservation law with source term

$$\begin{aligned} &U_t + F(U)_x = S(U), \\ &U(x,t^n) = U^n, \end{aligned} \tag{6.13}$$

can be solved numerically by splitting it into the homogeneous problem

$$\begin{aligned} &U_t + F(U)_x = 0, \\ &U(x,t^n) = U^n, \end{aligned} \tag{6.14}$$

and the source problem

$$\frac{dU}{dt} = S(U), \ U(0) = \bar{U}^{n+1}, \tag{6.15}$$

where $\bar{U}^{n+1}$ is the solution of the advection problem (6.14).

The Riemann problem (6.14) can be solved approximately by utilizing a conservative method of Godunov type to get

$$\bar{\mathrm{U}}_i^{n+1} = \mathrm{U}_i^n + \frac{\Delta t}{\Delta x}(\mathrm{F}^n_{i-\frac{1}{2}} - \mathrm{F}^n_{i+\frac{1}{2}}). \tag{6.16}$$

The ordinary differential equation (6.15) can be solved by using the methods for the numerical solution of the system of ordinary differential equations. In the present work we have employed the Euler method (See Toro (2009)). Thus the final solution of (6.13) is given by

$$\begin{aligned} \bar{U}_i^{n+1} &= U_i^n + \frac{\Delta t}{\Delta x}\left(F^n_{i-\frac{1}{2}} - F^n_{i+\frac{1}{2}} \right), \\ U_i^{n+1} &= \bar{U}_i^{n+1} + \Delta t S(\bar{U}_i^{n+1}), \end{aligned} \tag{6.17}$$

where U is the vector of conserved variables, $\bar{U}$ is the solution of the homogeneous equation, S is the source term and F is the numerical flux at the cell interface $i+1/2$ and $i-1/2$ given by

$$F^n_{i+\frac{1}{2}} = F\left(U^n_{i+\frac{1}{2}}(0) \right),\ F^n_{i-\frac{1}{2}} = F\left(U^n_{i-\frac{1}{2}}(0) \right), \tag{6.18}$$

where, $U^n_{i+\frac{1}{2}}(0)$ and $U^n_{i-\frac{1}{2}}(0)$ represents the solution of local Riemann Problem $RP\left(\mathrm{U}_i^n, \mathrm{U}_{i+1}^n\right)$ and $RP\left(\mathrm{U}_{i-1}^n, \mathrm{U}_i^n\right)$ respectively along the line $x/t = 0$.

6.5 HLLC method

Consider the figure 6.2, in which the whole of wave structure arising from the exact solution of the Riemann problem is contained in the control volume $[x_L, x_R]\times[0, \Delta t]$, that is

$$x_L \le \Delta t S_L,\ x_R \ge \Delta t S_R\ , \tag{6.19}$$

where S_L and S_R are the fastest signal velocities perturbing the initial data states U_L and U_R respectively, and Δt is the time step chosen.

Integrating the equation

$$\frac{\partial U}{\partial t}+\frac{\partial F}{\partial x}=0 \ , \tag{6.20}$$

in the control volume $[x_L, x_R]\times[0,\Delta t]$, we have

$$\int_{x_L}^{x_R} U(x,\Delta t)dx=\int_{x_L}^{x_R} U(x,0)dx+\int_{0}^{\Delta t} F(U(x_L,t))dt-\int_{0}^{\Delta t} F(U(x_R,t))dt \ ,$$

or

$$\int_{x_L}^{x_R} U(x,\Delta t)dt=x_R U_R-x_L U_L+\Delta t(F_L-F_R) \ , \tag{6.21}$$

which is the required consistency condition.

Splitting the integrals on the left hand side of (6.16) into four integrals, we get

$$\int_{x_L}^{x_R} U(x,\Delta t)dx=(\Delta t S_L-x_L)U_L+(x_R-\Delta t S_R)U_R+\int_{\Delta t S_L}^{\Delta t S_M} U(x,\Delta t)dx+\int_{\Delta t S_M}^{\Delta t S_R} U(x,\Delta t)dx \ . \tag{6.22}$$

Comparing equation (6.21) and (6.22), we have

$$\frac{1}{\Delta t(S_R-S_L)}\left[\int_{\Delta t S_L}^{\Delta t S_M} U(x,\Delta t)dx+\int_{\Delta t S_M}^{\Delta t S_R} U(x,\Delta t)dx\right]=\frac{S_R U_R-S_L U_L+F_L-F_R}{S_R-S_L} \ , \tag{6.23}$$

or

$$\left(\frac{S_M-S_L}{S_R-S_L}\right)U_L^*+\left(\frac{S_R-S_M}{S_R-S_L}\right)U_R^*=\frac{1}{\Delta t(S_R-S_L)}\int_{\Delta t S_L}^{\Delta t S_R} U(x,\Delta t)dx \ . \tag{6.24}$$

Integrating the equation (6.20) in the control volume $[x_L,0]\times[0,\Delta t]$, we obtain

$$\int_{\Delta t S_L}^{0} U(x,\Delta t)dx=-\Delta t\, S_L U_L+\Delta t(F_L-F_{0L}) \ , \tag{6.25}$$

where F_{0L} is the flux $F(U)$ along the $t-$axis. Solving for F_{0L} we find

$$F_{0L} = F_L - S_L U_L - \frac{1}{T}\int_{\Delta t S_L}^{0} U(x,\Delta t)dx \ . \tag{6.26}$$

Evaluation of the integral form of the conservation laws on the control volume $[0, x_R]\times[0,\Delta t]$ yields

$$F_{0L} = F_R - S_R U_R + \frac{1}{T}\int_{0}^{\Delta t S_R} U(x,\Delta t)dx \ . \tag{6.27}$$

It is easy to see that

$$F_{0L} = F_{0R} \ . \tag{6.28}$$

results in the consistency condition (6.21).

After several manipulations, the HLLC approximate solver is given as (Toro (2009))

$$U(x,t) = \begin{cases} U_L, \text{ if } \ x/t < S_L, \\ U_L^*, \text{ if } \ S_L \le x/t \le S_M, \\ U_R^*, \text{ if } S_M \le x/t \le S_R, \\ U_R, \text{ if } x/t \ge S_R. \end{cases} \tag{6.29}$$

with a corresponding HLLC numerical flux defined as (Toro (2009))

$$F_{i+1/2}^{HLLC} = \begin{cases} F_L, \text{ if } \ 0 \le S_L, \\ F_L^*, \text{if } S_L \le 0 \le S_M, \\ F_R^*, \text{if } S_M \le 0 \le S_R, \\ F_R, \text{if } 0 \ge S_R. \end{cases} \tag{6.30}$$

and the intermediate fluxes F_L^* and F_R^* as

$$F_K^* = F_L + S_K(U_K^* - U_K) \ , \tag{6.31}$$

for $K = L$ or $K = R$, with the intermediate states given as

$$U_K^* = \rho_K \left(\frac{S_K - u_K}{S_K - S_M}\right) \begin{bmatrix} 1 \\ S_M \\ E_K/\rho_K + (S_M - u_K)\left[S_M + p_K/(\rho_K(S_K - u_K))\right] \end{bmatrix}. \tag{6.32}$$

6.6 Wave speed estimates and time step size

For the computation of numerical fluxes, the selection of wave speed estimates is very important, as it has a great effect on the quality of numerical solutions. The direct wave estimates are the simplest methods providing maximum and minimum wave velocities. The simplest of them is the one suggested by Davis (1988)

$$S_L = u_L - a_L,\ S_R = u_R + a_R. \tag{6.33}$$

and

$$S_L = \min\{u_L - a_L, u_R - a_R\},\ S_R = \max\{u_L + a_L, u_R + a_R\}. \tag{6.34}$$

Einfeldt (1988) suggested to combine the estimates (6.34) with Roe average (Roe (1981)) eigenvalues for the left and right nonlinear waves, that is

$$S_L = \tilde{u} - \tilde{a}, S_R = \tilde{u} + \tilde{a}\ , \tag{6.35}$$

where $\tilde{u}$ and $\tilde{a}$ are the Roe average particle and sound speeds respectively, given as

$$\tilde{u} = (\sqrt{\rho_L}u_L + \sqrt{\rho_R}u_R)\big/(\sqrt{\rho_L} + \sqrt{\rho_R}),\ \tilde{a} = \left[(\gamma - 1)(\tilde{H} - \tilde{u}^2/2)\right]^{1/2}. \tag{6.36}$$

where the enthalpy $H = (E + p)/\rho$, is approximated as

$$\tilde{H} = (\sqrt{\rho_L}H_L + \sqrt{\rho_R}H_R)\big/(\sqrt{\rho_L} + \sqrt{\rho_R})\ . \tag{6.37}$$

A different approach for finding the wave estimate is based on pressure and was proposed by Toro (2009), given as

$$S_L = u_L - a_L T_L,\ S_R = u_R + a_R T_R\ . \tag{6.38}$$

with

$$T_K = \begin{cases} 1, & \text{if } p^* \le p_K \\ \left[1 + (\gamma+1)/(2\gamma)\left(p^*/p_K - 1\right)\right]^{1/2}, & \text{if } p^* > p_K \end{cases}, \tag{6.39}$$

where p^* is the pressure inside the unknown region. To use (6.38), we need an approxi-

mation of pressure inside the star region. The approximate value of pressure can be taken to be the PVRS approximation

$$\left.\begin{aligned} p_0 &= \max(TOL,\, p_{PV}) \\ p_{PV} &= (p_L + p_R)/2 + (\rho_L + \rho_R)(c_L + c_R)(v_L - v_R)/8 \end{aligned}\right\}. \tag{6.40}$$

Two shock approximation

$$\left.\begin{aligned} p_0 &= \max(TOL,\, p_{TS}) \\ p_{TS} &= \left(g_L(\overline{p})\,p_L + g_R(\overline{p})\,p_R - (v_R - v_L)\right)\Big/\left(g_L(\overline{p}) + g_R(\overline{p})\right) \\ g_K(p) &= \left[A_K \Big/ \left(p + B_K\right)\right]^{1/2} \end{aligned}\right\}. \tag{6.41}$$

Two rarefaction approximation

$$p_{TR} = \left[\frac{c_L + c_R - (\Gamma - 1)(v_R - v_L)}{c_L/(p_L)^{(\Gamma-1)/2\Gamma} + c_R/(p_R)^{(\Gamma-1)/2\Gamma}}\right]^{2\Gamma/(\Gamma-1)}. \tag{6.42}$$

In the present paper, we have used the estimates given as

$$S_L = \min\left\{\tilde{u} - \tilde{a}, u_L - a_L T_L\right\}, \tag{6.43}$$

$$S_R = \max\left\{\tilde{u} + \tilde{a}, u_R + a_R T_R\right\}, \tag{6.44}$$

where $\tilde{u}$, $\tilde{a}$ are given in (6.36) and T_L, T_R are given in (6.39).

The intermediate speed S_M in terms of S_L and S_R are given as

$$S_M = \frac{p_R - p_L + \rho_L u_L (S_L - u_L) - \rho_R u_R (S_R - u_R)}{\rho_L (S_L - u_L) - \rho_R (S_R - u_R)}. \tag{6.45}$$

The choice of the size of the time step Δt in the conservative problem is related to the stability condition of the particular scheme. It depends on the method considered, the grid spacing and the wave velocity. It is given as

$$\Delta t = C_{cfl}\,\Delta x \Big/ S^n_{i,j\,\max}. \tag{6.46}$$

where $S^n_{ij\,\max}$ is the wave of maximum velocity at a particular time level.

6.7 Numerical Example

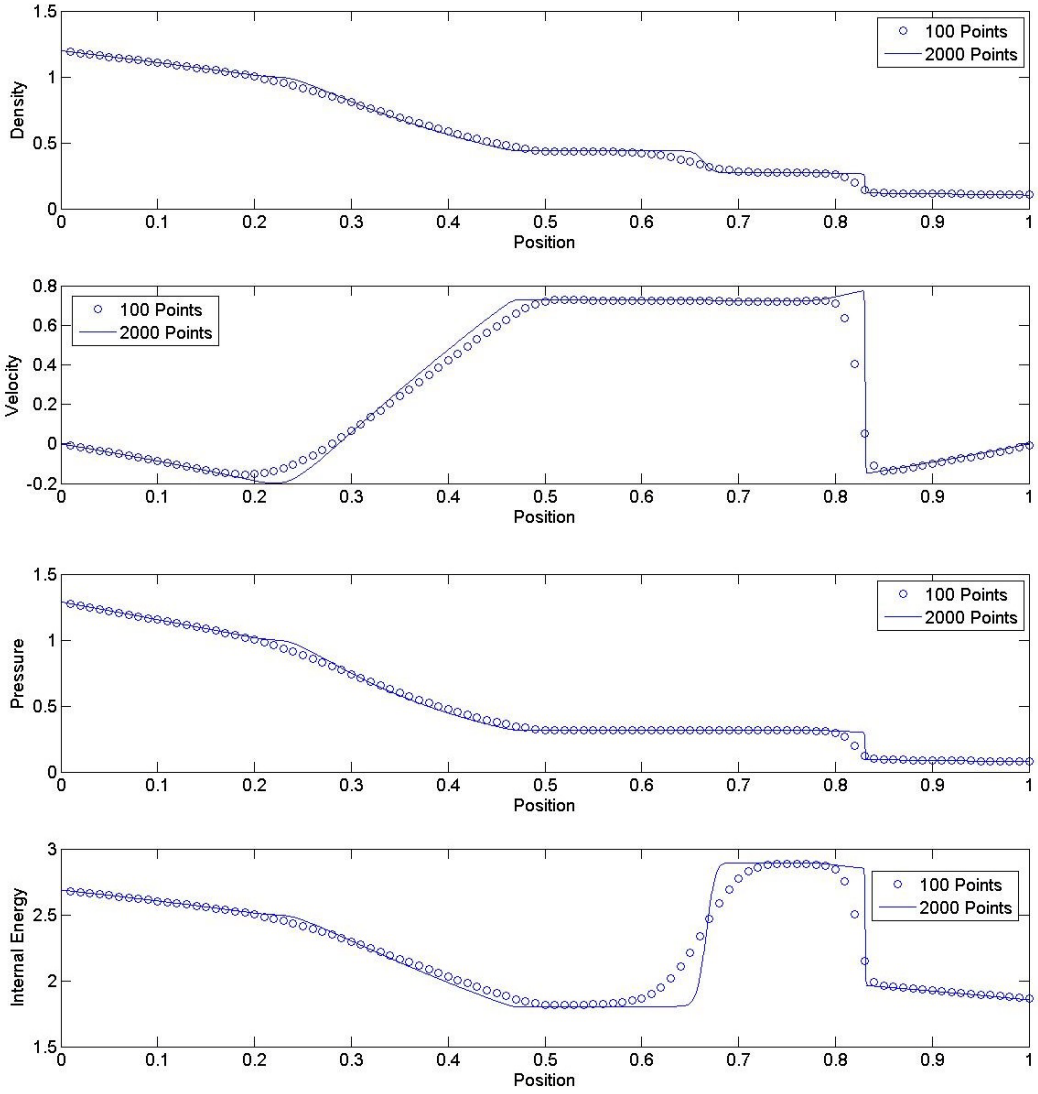

Figure 6.3 Density, velocity, pressure and internal energy profiles for test 1 with 100 and 2000 grid points.

The data for the two test problems considered in the present work are given in table 1. In both the test problems the domain under consideration is [0, 1] and the initial conditions are given as

$$(\rho, u, p) = \begin{cases} (\rho_L, u_L, p_L), & x < 1/2, \\ (\rho_R, u_R, p_R), & x > 1/2. \end{cases} \tag{6.47}$$

In all cases the ratio of specific heats is taken to be $\gamma = 1.4$. The solution is computed using solid wall boundary conditions. Test 1 is the standard Sod test problem together with gravitational field, taken as in Xing et. al. (2013) and Chandrashekar et. al. (2015). Test 2 studies the contact discontinuity under the gravitational field. The data for test 2 is same as given in Chandrashekar et. al (2015).

Test	ρ_L	v_L	p_L	ρ_R	v_R	p_R	$\phi(x)$
1	1.0	0.0	1.0	0.125	0.0	0.1	x
2	1.0	-2.0	0.4	1.0	2.0	0.4	x

Table 6.1 Data for the test problems

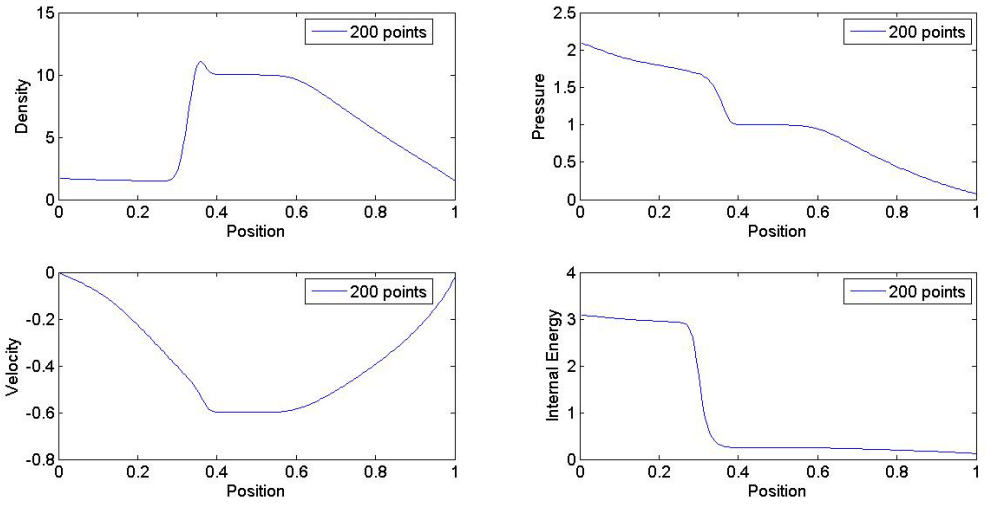

Figure 6.4 Solution profile for test 2 with 200 cells

6.8 Result and Discussion

For the test 1, the solutions are obtained for 100 and 2000 cells until a time of $t = 0.2s$ and the solution profiles for density, velocity, pressure and internal energy are shown in the figure 6.3. From figure 6.3, we see that the coarse mesh with 100 grid points is able to resolve all the features in the solution without having spurious

oscillations. It can be seen that density increases near $x = 0$ due to the gravitational force which is directed to the left. The present test indicates that the application of the HLLC solver with operator splitting preserves the non-oscillatory nature of the solution. The results are in agreement to those obtained in Chandrashekar et. al (2015). Figure 6.3 clearly shows the effect of gravitational potential. In the absence of gravitational field, the solution results in three waves, a left rarefaction wave, a middle contact discontinuity and a right shock wave. Test 2 is the 1-D contact case. The results obtained with our scheme on meshes with 200 cells are shown in figure 6.4. In figure 6.5, the solutions are computed with 2000 cells. The results are in close agreement with those obtained in Chandrashekar et. al (2015). Moreover, we again observe that the solutions are non-oscillatory at the discontinuities.

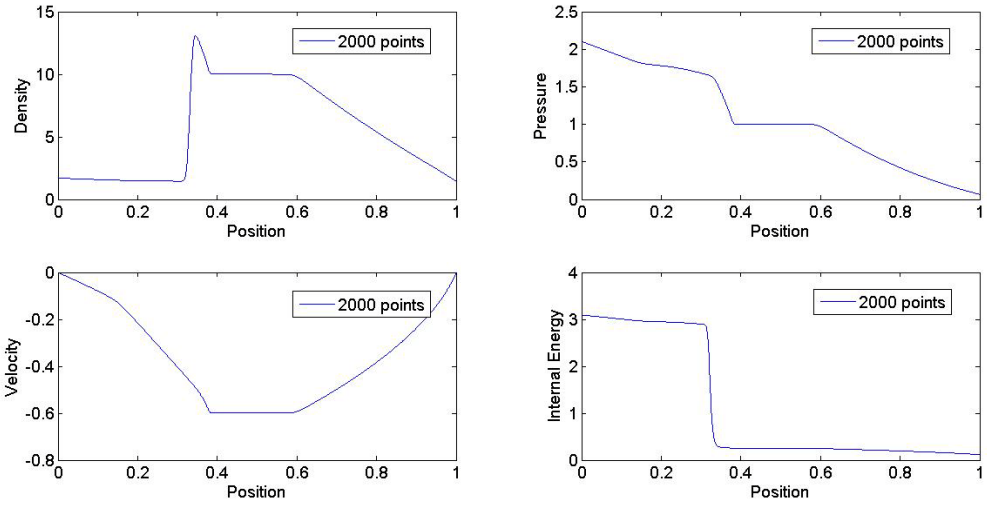

Figure 6.5 Solution profile for test 2 with 2000 cells